IEEE Access
Multidisciplinary | Rapid Review | Open Access Journal

Received December 2, 2020, accepted December 13, 2020, date of publication December 24, 2020, date of current version February 1, 2021.

Digital Object Identifier 10.1109/ACCESS.2020.3047127

A Nearly Optimal Method of Polar Code Constructions for the AWGN Channel

HAICHAO SUN[1,2], YANJIE WANG[1,2], RUI TIAN[1], AND HONGWEI ZHAO[3]

[1]Changchun Institute of Optics, Fine Mechanics and Physics, Chinese Academy of Sciences, Changchun 130033, China
[2]University of Chinese Academy of Sciences, Beijing 100049, China
[3]College of Computer Science and Technology, Jilin University, Changchun 130012, China

Corresponding author: Rui Tian (tianrui_81@aliyun.com)

This work was supported in part by the National Natural Science Foundation of China under Grant 61401425, in part by the Provincial Science and Technology Innovation Special Fund Project of Jilin Province under Grant 20190302026GX, and in part by the Natural Science Foundation of Jilin Province under Grant 20200201037JC.

ABSTRACT Polar code is a kind of capacity-approaching code with explicit structure as part of the next generation wireless communication standard. The performance of the polar code is directly determined by the construction method, in which there are three important parameters: code rate (R), block-length (N), and designSNR ($DSNR$). It is very difficult to obtain an optimal construction because all these three parameters should be optimized in a recursive structure model. In this article, an efficient method, which constructs the desired optimal polar code by simultaneously selecting the three parameters in terms of the error probability, is presented. In the proposed construction, a dimensionality reduction search method is used to solve a fore mentioned optimization problem and to find the relation between the performance of polar code and design parameters. At the same time, the optimal parameters N and R can be obtained under any $DSNR$ by taking the average group accuracy rate as the evaluation criterion. Through this method, the appropriate solution of three parameters in the construction of the polar code can be determined according to the required error probability. The proposed construction method is verified by numerical simulation, and the optimal performance to N, R and $DSNR$ is compared and discussed.

INDEX TERMS Polar code, Gaussian approximation, ABLCR, dimensionality reduction.

I. INTRODUCTION

Polar code, constructed by using channel polarization with encoding and decoding complexity $O(\mathrm{Nlog_2N})$ is the first one proved to achieve Shannon's symmetric capacity in Binary-input Discrete Memoryless Channel (B-DMC). Compared with other encoding methods such as turbo codes and low-density parity-check (LDPC) codes [1]–[3], polar code takes great advantages in short block length and addresses a latency issue of successive cancellation decoding. Also, it has been applied in the fifthgeneration (5G) wireless communication systems in [4]–[11] In 2016, polar code became the final solution for enhanced mobile broadband (eMBB) scene of the 5G control channel.

During the polar code construction process, code rate (R), block-length (N), error probability (pe) and the quality of the channel (W) are of interest to us Moreover, the quality of the channel can be expressed as its capacity I (W) or its Bhattacharyya parameter Z(W) in different methods and channels To quantize the channel, especially the Additive White Gaussian Noise(AWGN) channel, the specified value of signal-to-noise ratio (SNR), which is known as design-SNR($DSNR$), dictates the generation of the polar codes due to the nonuniversality of these codes. As [12] mentioned, the polar code has a nonasymptotic structure. For this reason, [13], [14] concluded that it is a consensus that the extraction of formulation for these critical parameters is very difficult. Although the classic polar code construction methods [15]–[19] demonstrate that the defect of algorithm complexity is solved and it is applicable to a variety of channels, there is no further research on the problem of formulating the exact description of the parameters In recent years, more and more researches have been carried out in this field by simplifying this problem, but only studying the relationship between other parameters when some parameters are fixed. As [20]–[22] presented in order to design a universal polar code, which is not constrained by $DSNR$, the study of the partial order is effective for engineering practical applications.

The associate editor coordinating the review of this manuscript and approving it for publication was Ali Afana.

This work is licensed under a Creative Commons Attribution 4.0 License. For more information, see https://creativecommons.org/licenses/by/4.0/

Another option to tackle this problem is to consider the relationship between the error probability and the blocklength with the remaining parameters fixed. Such as Arikan *et al.* demonstrated in [23], the upper bound of the block error probability under a binary-input memoryless symmetric (BMS) channel when the rate is fixed and N is large enough. Moreover, a more accurate result is given to this upper bound in [24] Furthermore, [25] gives the mathematical relationship between the error probability and the code length N with a fixed rate. Also, some other scholars have studied the relationship between the block-length and the rate while fixing other parameters. For example, [12], [24], [26] show that the minimum possible block-length N is required to achieve a rate R with a fixed error probability. Meanwhile, [13] describes that the relationship between the block length and the rate when the error probability is fixed, and it is applicable to all BMS channels In addition, [14] gives tighter upper bound for the scaling exponent when the quality of the channel W and the error probability are fixed. In 5G standard the method of selection parameters depends roughly on the quantity and type of information data A mother polar code of length $N = 2^n$ is calculated as:

$$n = \max(\min(\mathrm{n}_1, \mathrm{n}_2, \mathrm{n}_{up}), \mathrm{n}_{low}) \tag{1}$$

where n_{low} and n_{up} give a lower and an upper bound on the mother code length, and $n_2 = \log_2(8K)$, $n_1 = \log_2(E)$ Where E is the codeword length and K is the length of information bits Therefore, when using these algorithms or methods to guide and design polar code structures, the fixed parameters can only be roughly designed based on experience or simple strategies, such as in 5G application, which solves this problem in the rate matching step This is obviously not accurate enough, at least not optimal and the performance of polar code is reduced in this way, because of the lack of the impact of fixed parameters on performance. The main motivation of this article is to use the shortest N under the expected error probability to find the optimal polar code construction method by all parameters The proposed algorithm avoids the direct theoretical derivation of other algorithms, and is a traversal search algorithm, which can accurately obtain the relationship between all design parameters and performance. Thus, an approximately optimal polar code structure is constructed

In practice, it is desirable that the constructed polar code has the required block-length N and the rate R with a desired error probability. Meanwhile, the shortest encoding length is of great interest in terms of the rate R and a wider adaptation range of possible SNRs The shorter the N, the smaller the resource is required for realizing the polar code construction, and the faster the encoding and decoding speed will be. In order to achieve the above objectives, a dimensionality reduction polar code construction algorithm was implemented. Firstly a simulation model of the channel was established. Secondly according to Gaussian approximation theory, which can characterize the performance of the coding, the average block correct rate was obtained. Finally, a simple search algorithm, which can find the relationship between the code performance and polar code construction parameters is put into effect. As a result the optimal polar code construction algorithm among all the parameters can be acquired. The relationship obtained in this way is particularly beneficial to the selection and dynamic adjustment of the parameters in the polar code construction. To verify the effectiveness of the algorithm, the encoding process and the decoding process of the polar code were simulated, and the results show the consistency between the algorithm proposed in this article and the Monte Carlo algorithm. The performance is also better than the polar code structure in the 5G standard

II. PRELIMINARIES

In this section, some useful notations and definitions, which will be used in the sequel, are presented.

A. NOTATION

Polar codes are constructed based on a phenomenon called channel polarization by combining and splitting. As the block-length N increases, the polarization phenomenon occurs and the reliability of some channels will increase, while others will decrease. The construction of polar code is the selection of the best K bit-channels as information bits and the worst N-K bit-channels as frozen bits among N The code rate(R) is equal to K/N

Let $u_1^N = (u_1, u_2, \cdots, u_N)$ be the input bit vector and $x_1^N = (x_1, x_2, \cdots, x_N)$ be the output bit vector. The input vector u_1^N consists of the K information bits and the $N - K$ frozen bits. The mapping $u_1^N \to x_1^N$ denotes $x_1^N = u_1^N G_N$ by a matrix G_N. G_N is the generator matrix of polar code and there is a formula for $G_N = B_N F^{\otimes n}$ where respects bit-reversal operator $F^{\otimes n} = F \otimes \cdots \otimes F$ (n copies), $F = \begin{pmatrix} 1 & 0 \\ 1 & 1 \end{pmatrix}$, and $\otimes n$ denotes the Kronecker power

B. SIMULATION MODEL

A typical communication system model including channel coding operations is shown in Fig.1. In the transmitter, the K information bits are encoded with a polar code as N encoded bits. These bits are modulated with Binary Phase Shift Keying (BPSK) modulation, respectively. Then, the modulated symbols are transmitted over the AWGN channel. At the receiver, the reverse processes, including BPSK demodulation, successive cancellation (SC) decoding perform channel decoding task to reconstruct the information bits by removing noise

In an AWGN channel, the modulated signal s(t) has noise n(t) added to it prior to reception. The noise n(t) is a white Gaussian random process with mean $2/\sigma^2$ and variance $4/\sigma^2$, where σ^2 is equal to power spectral density (PSD) N0/2. The received signal is thus r(t) = s(t) + n(t). The received *SNR* is defined as the ratio of the received signal power to the noise power within the bandwidth of the transmitted signal s(t). Since the noise n(t) has uniform PSD N0/2, the total noise power within the bandwidth 2B is N = N0/2 · 2B = N0 · B.

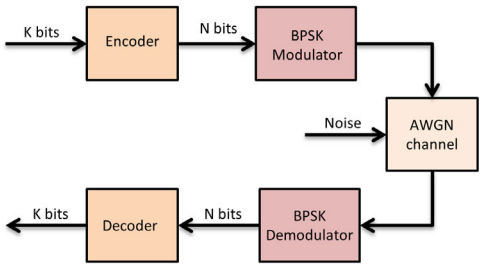

FIGURE 1. The typical communication model.

Hence the received *SNR* is given by $SNR = \frac{P_r}{N_0 B} = \frac{E_o}{N_0 B T_0} = \frac{E_b}{N_0 B T_b}$, where E_s is the symbol energy and E_b is the bit energy. For pulse shaping with Tb = 1/B (e.g., raised cosine pulses equal 1), there is $SNR = \frac{E_b}{N_0}$ for binary signaling. According to the principle of conservation of transmission symbol energy, the relationship between EsN0 and EbN0 can be described as follows:

$$\frac{Es}{N0} = f * \frac{Eb}{N0} = R \cdot \log_2 M * \frac{Eb}{N0} \tag{2}$$

where f is the number of information bits per symbol, which might be influenced by the size of the modulation alphabet (M-ary signaling) or the code rate of an error-control code (R). To simplify simulation, bits in the signal s(t) are modulated by BPSK Here M=2 and

$$\frac{Es}{N0} = R^* \frac{Eb}{N0} = R^* SNR \tag{3}$$

Usually, the energy per symbol is set equal to 1, $\frac{1}{N_0} = \frac{1}{2\sigma^2} = R^*$ SNR. Therefore, the code rate R and *SNR* are inversely proportional in a specified mean Gaussian channel

III. ANALYSIS OF RELIABILITY ESTIMATION

In an AWGN channel, the noise distribution is $N \sim (0, \sigma^2)$ according to [27]–[30]. When indicating an input signal and an output signal, 0 and 1 are expressed by $+1$ and -1 with BPSK modulation; therefore 1-2x indicates the modulation signal. When n is the noise signal, the probability density function is expressed as:

$$P(n) = \frac{1}{\sqrt{2\pi\sigma^2}} \exp\left(-\frac{(n)^2}{2\sigma^2}\right). \tag{4}$$

So we can get the conditional probability

$$P(y \mid x = 0) = \frac{1}{\sqrt{2\pi\sigma^2}} \exp\left(-\frac{(n-1)^2}{2\sigma^2}\right) \tag{5}$$

and

$$P(y \mid x = 1) = \frac{1}{\sqrt{2\pi\sigma^2}} \exp\left(-\frac{(n+1)^2}{2\sigma^2}\right) \tag{6}$$

It can be obtained that the Log-Likelihood Ratio (*LLR*) message of every bit channel by properties of conditional probability

$$L(y) = \ln \frac{P(y \mid x = 0)}{P(y \mid x = 1)} = \frac{2y}{\sigma^2}. \tag{7}$$

Hence $L(y)$ is also a Gaussian distribution $N(\frac{2}{\sigma^2}, \frac{4}{\sigma^2})$ According to the recursive structure of the polar code, the results of the two convolution operations performed by the probability density functions of the two Gaussian distributions are very similar to the distributions. Since the Gaussian distribution can only be expressed by the mean variance and there is a two-fold relationship between the variance and the mean, therefore the *LLR* follows a Gaussian distribution that is only related to the mean of the Gaussian distribution. Assuming the mean is $E[L_N^{(i)}]$ the calculation of the *LLR* is converted into a recursive process of the mean:

$$E\left[L_N^{(i)}\right] = \phi^{-1}\left(1 - \left(1 - \phi\left(E\left[L_{N/2}^{(i+2)/2}\right]\right)\right)\right)^2, \tag{8}$$

$$E\left[L_N^{(i)}\right] = 2E\left[L_{N/2}^{(i/2)}\right], \tag{9}$$

$$E\left[L_1^{(1)}\right] = \frac{2}{\sigma^2}, \tag{10}$$

where

$$\phi(x) \triangleq 1 - \frac{1}{\sqrt{4\pi x}} \int_{-\infty}^{\infty} \tanh\left(\frac{\tau}{2}\right) e^{-\frac{(\tau - x)^2}{4x}} d\tau$$

The simplified way demonstrated in [30] is

$$\phi(x) = \begin{cases} e^{-0.4527\, e^{0\times 6} + 0.0218}, & 0 < x < 10 \\ \sqrt{\frac{\pi}{x}} e^{-\frac{e}{4}} \left(1 - \frac{10}{7x}\right), & x \geq 10 \end{cases} \tag{11}$$

Thus, the probability density function of each channel is obtained, and then the error probability of each sub channel is acquired with SC decoding.

$$P(C_i) = \frac{1}{2} erfc\left(0.5\sqrt{E\left[L_N^{(i)}\right]}\right), \tag{12}$$

$$erfc(x) = (2/\sqrt{\pi}) \int_x^{\infty} e^{-\eta^2} d\eta. \tag{13}$$

According to the theory of the polar code constructed by Gaussian approximation, the block error rate can be obtained, which is expressed as:

$$P(\varepsilon) = 1 - P_r\left(\varepsilon^c\right) = 1 - \prod_{i \in \Gamma} \left(1 - P(C_i)\right), \tag{14}$$

then the block correct rate (BCR) is $P_{bcr}(\varepsilon^c = \prod_{i \in \Gamma}(1 - P(C_i))$ The block correct rate of the polar codes with different N and K is redefined as $P_K(N)$. If the length of each transmitted data is L, the data will be divided into L/K blocks. The total correct probability can be expressed as:

$$P_c(L) = P_K(N)^{L/K}. \tag{15}$$

After normalization, it can be considered that L is 1, and take the logarithmic transformation on both sides of the equation to get the average block correct rate (ABLCR)

$$C_{ablcr}(K) = \frac{\ln P_K(N)}{K}. \tag{16}$$

The average block correct rate indicates the average correct probability of each bit. The block correct rate of data is the

sum of their average block correct rates. Also, the sum of the block error rate and the block accuracy rate is 1. Therefore, the average block accuracy rate can be used to evaluate the coding performance, which is like the concept of the bit error rate. If the specified block error probability of polar code is (15), the required average block correct probability is (16).

According to the theory of polar codes in [16], when the code length increases, some channels tend to be perfect channels with a capacity close to 1 (no errors), and other channels tend to be pure noise channels with a capacity close to 0. Therefore, if the channels are reordered by the error probability according to the steps in the polar code construction, a typical sigmoid function will be obtained. The error probability of the i-th bit channel can be approximately expressed as:

$$\mathrm{P}(\mathrm{C}_i) = \alpha + \frac{\kappa}{1 + (\chi_i/\nu)^{\beta}}, \quad \chi_i = i/N \tag{17}$$

According to the nature of the polar code, the lower bound of the error probability is close to 0, which is $\mathrm{P}(C_i) = 0$. So $\alpha \approx 0$ is obtained. At the same time, when $i \to 1$, the upper bound of the error probability approximately equals to κ by (17). According to (12), the LLR corresponding to the largest error probability is also the smallest. Formula (8) approximately diverges within a certain range in the iterative process, while (9) converges. Therefore, the smallest *LLR* is n-1 iterations of (8). When the iterative transformation of (8) is expressed as H, the smallest *LLR* is

$$LLR^{\min} = H^n(\sigma^2). \tag{18}$$

Then

$$\kappa = P(LLR^{\min}), \tag{19}$$

is obtained, where $1/\sigma^2 = 2 * R * 10^{0.1 * DSNR}$. When $\nu = \chi_i$, it is clear that $P(C_i) = \kappa/2$ from (17). It shows that when the error probability is $\kappa/2$, the corresponding χ_i is equal to ν. The calculation process can be expressed as

$$P^{-1}(\kappa/2) = LLR_i, \tag{20}$$

$$\nu = i/N. \tag{21}$$

As the code length N increases, the polarization phenomenon becomes more serious. Therefore, the parameter β in (17) is a function of N, where

$$n = \log_2(N). \tag{22}$$

Then (17) can be simplified to

$$\mathrm{P}(C_i) = \frac{\kappa}{1 + (\frac{\chi_i}{\nu})^n}, \tag{23}$$

According to (19) (21)and (22), the parameters $\kappa(\sigma^2, N)$, $\nu(\sigma^2, \mathrm{N})$ and n can be determined. So according to (14) and (16), it can be obtained that the approximate estimation function (AF) for the average block correct rate about σ^2, N and K, as $C_{ablcr}(\mathrm{K}) = \varphi(\sigma^2, \mathrm{N}, \mathrm{K})$. In Fig.2, the approximate estimation function (AF) and the error probability calculation method (EPC)by (12) in the polar code construction are compared. The estimation of the upper and lower bounds of AF is relatively accurate. In table 1, the root mean squared error (RMSE) of AF is less than 3% and the coefficient of determination (R-square) of AF is greater than 90%. In addition, if the parameter β is more accurate, the accuracy of the two arcs in the sigmoid function will be improved, thereby improving the estimation accuracy of AF in Fig.2.

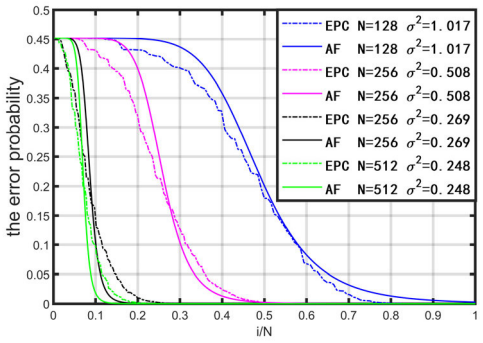

FIGURE 2. The comparison of the error probability of AF and EPC.

TABLE 1. Error of the approximate estimation function.

(N, σ^2)	(128,1.017)	(256,0.508)	(256,0.269)	(512,0.248)
RMSE(%)	2.08%	2.54%	2.57%	2.24%
R-square (%)	98.77%	97.66%	93.77%	94.78%

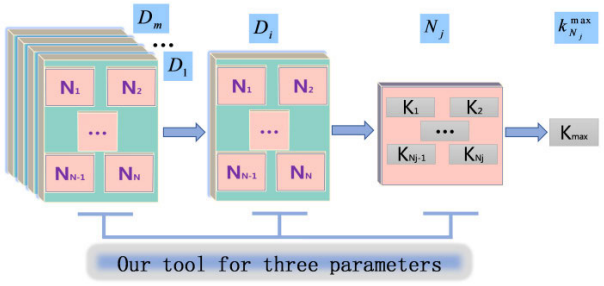

FIGURE 3. The steps of ABLCR calculation method.

IV. POLAR CODE CONSTRUCTION ALGORITHMS

By calculating the reliability of each channel, the error probability of each bit channel can be acquired, and the average block correct rate can be obtained. The ABLCR is used to evaluate the performance of different polar codes. For the construction of a polar code with a specified block error rate (BLER), the BLER can be converted into an ABLCR rate by an expression $C_{ablcr}(k) = \ln(1 - P_e)/K$. The problem of the polar code construction is how to choose the three parameters (*N, K, DSNR*) where *DSNR* is the design-SNR Firstly some definitions will be introduced in this paragraph. A set of DSNRs $\{D_1, D_2 \cdots D_m\}$ covers the range of DSNRs

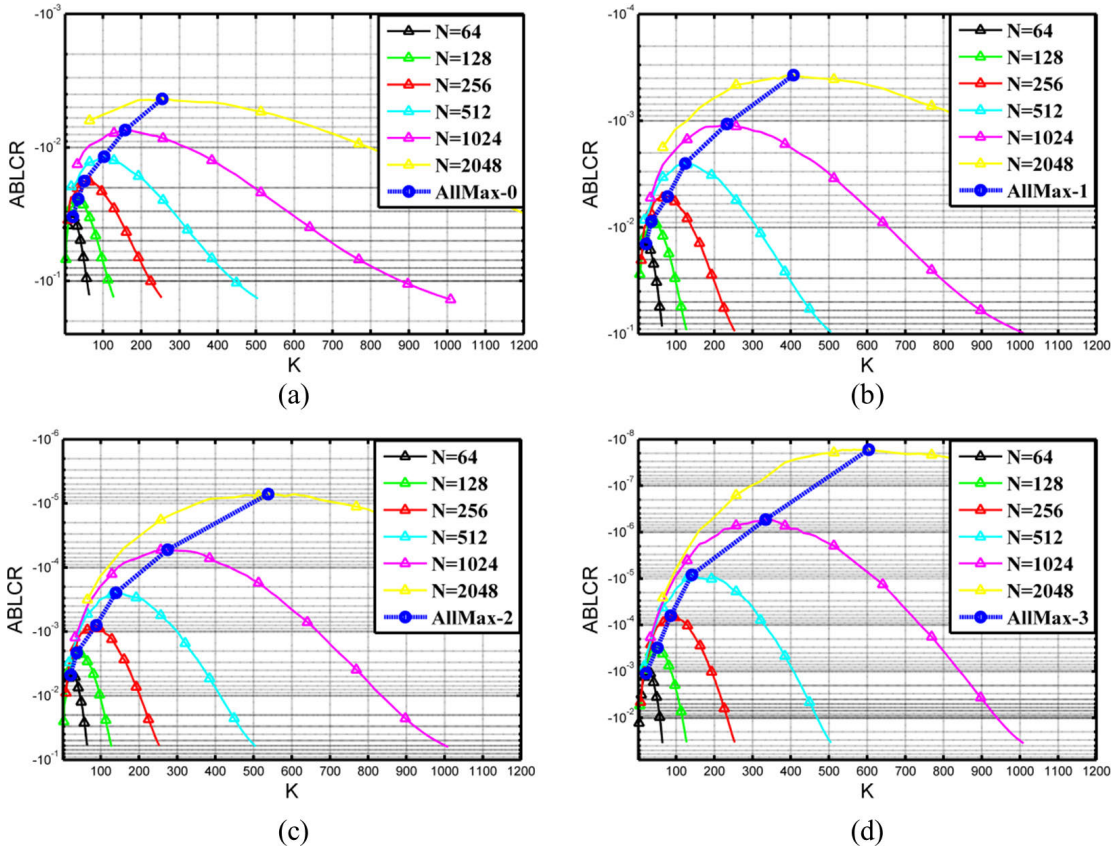

FIGURE 4. The ABLCR of different code length N when DSNR is one specified value. (a) DSNR = 0. (b) DSNR = 1. (c) DSNR = 2. (s) DSNR = 3.

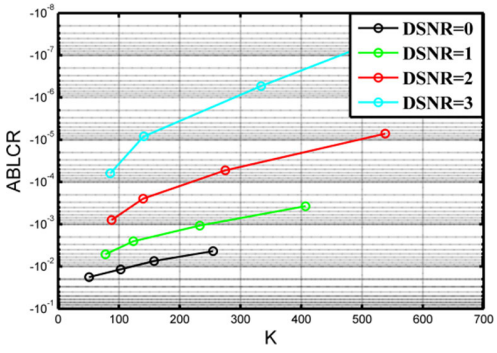

FIGURE 5. The curves of the set of maximum ABLCR s at different DSNRs.

of interest and $D_i \in \{D_1, D_2 \cdots D_m\}$. The range of selected encoding length is $N_i \in \{N_1, N_2 \cdots N_p\}$ and $N_j = 2^{n_j}$. For polar codes of each encoding length N_j the selection range of effective information bits is $K_{N_j} \in \{1, 2, \cdots N_j\}$.

The algorithm steps and principles in Fig.3 are presented as follows:

1) Through the method of section III, the sets of ABLCR can be obtained from

$$\Lambda_{(D_i,N_j)} = \left\{ C_{(D_i,N_j)}\left(k_{N_j}\right) : k_{N_j} = 1, 2, \ldots, N_j \right\}$$

with fixed parameters (D_i, N_j). It can be seen from Fig.4(a)-(d) that $\Lambda_{(D_i,N_J)}$ is an approximate discrete quadratic

Function `Calculate_ABLCR` (N_j, D_i) **is**
  input: N_j code length, D_i DSNR in dB
  output: $\max[\Lambda_{D_i,N_j}]$ the maximum value of ABLCR
  $n_j = log_2^{N_j}$;
  k_{N_j} *is the information bit length;*
  for $k_{N_j} = 1$ **to** N_j **do**
    Initialize LLRs mean values $E[L_o^{(0)}] = 4(N_j/k_{n_j}) * D_i$;
    for $r = 1$ **to** n_j **do**
      $U = 2^r$;
      for $t = 0$ **to** $\frac{u}{2} - 1$ **do**
        $T = E[L_{r-1}^{(t)}]$;
        $E[L_r^{(t)}] = \phi^{-1}(1 - (1 - \phi(T)))^2$;
        $E[L_r^{(t+u/2)}] = 2T$;
      end
    end
    Get the ABLCR $C_{(D_i,N_j)}(k_{N_j})$ *by the error probability of* k_{N_j} *information bits*;
  end
  Get the sets of ABLCR $\Lambda_{(D_i,N_j)} = \{C_{(D_i,N_j)}(k_{N_j}) : k_{N_j} = 1, 2, \ldots, N_j\}$;
  return $\max[\Lambda_{(D_i,N_j)}]$;
end

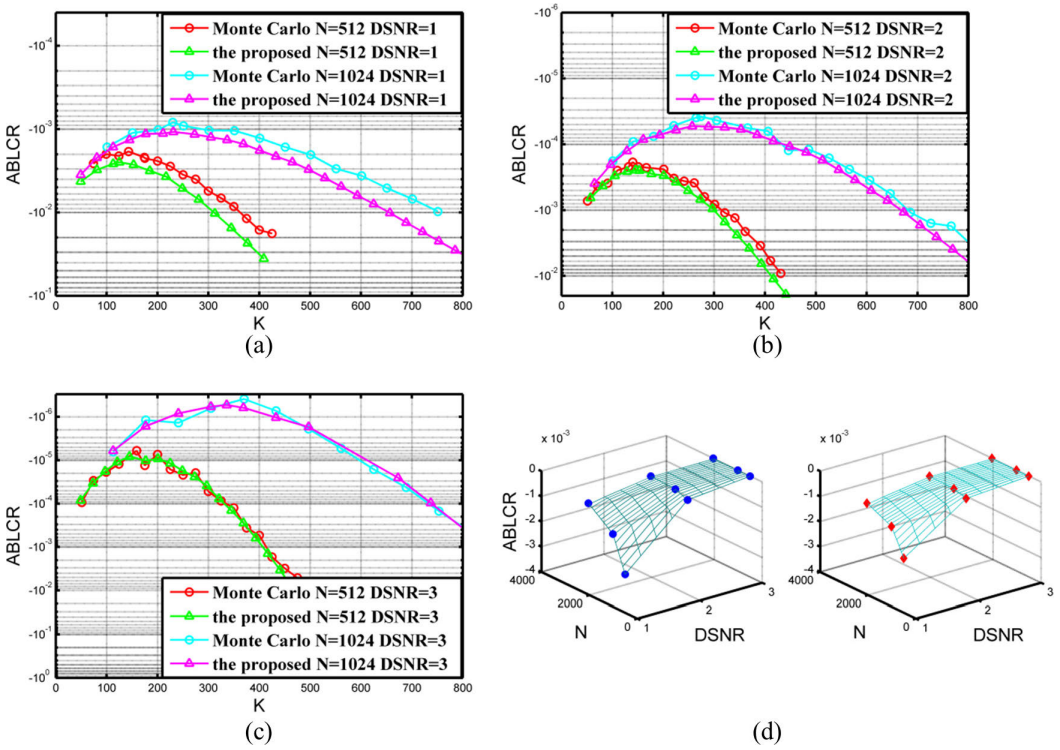

FIGURE 6. ABLCR comparison of the proposed method and Monte Carlo's method when N=512 and N=1024 by different DSNRs in (a),(b)and(c). (a) DSNR=1. (b) DSNR=2. (c) DSNR=3. (d) the ABLCR maximum of different DSNRs and different code length by the proposed method and Monte Carlo's method.

curve function and its maximum value is $\max[\Lambda_{(D_i,N_j)}] = C_{(D_i,N_j)}(k_{N_j}^{\max})$ When N is N_j and $DSNR$ is D_i, $k_{N_j}^{\max}$ is is the number of information bits corresponding to the maximum value of ABLCR. Consequently, a polar code, which is under the maximum of ABLCR, can be constructed by puncturing or shortening techniques mentioned in [31]–[34]. In this way, a single maximum point can be used to represent the function curve and achieve the dimensionality reduction expression of ABLCR. This method is effective to divide the three-parameter selection into two steps: the first step is to select $DSNR$ and N, and the second step is to select valid information bit K.

2) When $DSNR$ is D_i, the sets of maximal ABLCR can be acquired from

$$\Upsilon_{D_i} = \left\{ \max[\Lambda_{(D_i,N_1)}], \max[\Lambda_{(D_i,N_2)}], \ldots \max[\Lambda_{(D_i,N_p)}] \right\}$$

by calculating all the maximum value with different N_j. Then draw all the sets of Υ_{D_i}, $\Omega = \{\Upsilon_{D_1}, \Upsilon_{D_2}, \cdots \Upsilon_{D_m}\}$ as illustrated in Fig.5. The calculation ABLCR algorithm is shown in Function Calculate_ABLCR (N_j, D_i). In this way, the relation chart between the ABLCR and (N, K, $DSNR$) can be achieved. This chart can be used as a tool to select three parameters.

3) The desired error probability for $BLER$ is converted into ABLCR by formula(16).

4) According to the desired ABLCR, the appropriate D_i and as illustrated in Fig. can be chosen from Fig.5. Generally, the small D_i and minimum code length N_J is picked out to reduce the complexity of the polar code as much as possible.

5) According to the selected D_i and N_j the discrete quadratic curve function can be determined from Fig.4(a)-(d). Thus $k_{N_j}^{\max}$ can be confirmed.

The proposed algorithm finally obtains the relation chart between the ABLCR and all design parameters within the search range. Meanwhile, the optimal design parameters can be obtained in this range according to the desired ABLCR. Moreover, the result obtained by the proposed algorithm is a standard look-up table and exempt from recalculating, hence the algorithm has great practical value. The complexity of the proposed algorithm is $O(\mathrm{m}^*\mathrm{N}_p^* \log(\mathrm{N}_p))$, where m is the total number of DSNRs of interest, and N_p is the maximum code length.

V. SIMULATIONS AND DISCUSSION

In this section, firstly, the simulation results of the ABLCR from the code length 2^6 to 2^{11} and $DSNR$0dB to 3dB are illustrated in Fig.4. Also, it can be seen that the ABLCR with K is an approximate quadratic curve and has the maximum value. The reason for this phenomenon is due to the waste of channel capacity when the number of information bits is very small. Although the reliability is high, the transmission rate is lower As a result, the ABLCR is at a low level. As the number of information bits increases and the transmission rate raises, the ABLCR will improve continuously. After the ABLCR reaches the maximum value, it starts to decline, because the reliability of the later information bits decreases while the number of them increases. Thus, the curves of the set of

maximum ABLCRs are shown in Fig.4. Then, $C_{(D_i,N_j)}(k_{N_j}^{\max})$ under different DSNRs ranging from 0dB to 3dB is shown in Fig.5. The similar results as [35] describes, i.e., the smaller the *DSNR* the better the overall performance, can be discovered. When selecting *DSNR* parameters, the method in [35] can also be the reference to verify the bit error rate (*BER*) performance of the constructed polar codes in other SNRs.

Moreover, the following rules were concluded for the ABLCR of each construction method with one code length:

(1) There is a range between the maximum and the minimum values for ABLCR.

(2) There is a maximum value for the average block correct rate. If the code lengths are the same, the larger *DSNRs* corresponds to the higher maximum ABLCR values as illustrated in Fig.5.

(3) When the code length is longer, the range is wider, and the maximum ABLCR value is higher as shown in Fig.4(a)-(d). Therefore, short codes can replace long codes within a certain range. The theory is proved in [12] that as the code length increases, polar code will continue to achieve the capacity of binary input channels, and the reliability of the selected information bit is higher.

Furthermore, the Monte Carlo method is an algorithm that simulates a typical communication system model in Fig.1 It uses the Gaussian approximation algorithm to encode and the SC algorithm to decode in the Gaussian white noise channel. The Monte Carlo method was utilized to verify the correctness of the proposed algorithm. Fig.6(a)-(c) shows the ABLCR performance comparison between the proposed method and the Monte Carlo method. It can be clearly seen from Fig.6(a), especially from Fig.6(b)-(c), that the performance calculated by the proposed method is basically consistent with the Monte Carlo method.

Also, the set of maximum ABLCRs at different DSNRs in Fig.5 is fundamentally concordant with Fig.4(a)-(d). Meanwhile, in Fig.6(a), when the effective information bits K is the same, the ABLCR value is higher, i.e. showing better performance. There is no manifested difference between the Monte Carlo method and the proposed method. Consequently, this will not affect the selection of effective information bit K by the proposed method because the effective information bit K of the maximum ABLCR value by the two methods is almost identical. In addition, it can be considered that the parameters selected by the proposed method have a performance margin. In other words, when different code lengths and DSNRs are selected, the maximum values of ABLCRs are essentially identical as illustrated in Fig.6(d), and the error of the corresponding valid information bit $K_{\max}$ is below 4% as listed in Table 2. Thereby, the corresponding optimal performance and the corresponding effective information bit K are also almost similar between the Monte Carlo and the presented method. Therefore, the appropriate parameters DSNR, N and K can be chosen to get the optimal performance by the proposed method for constructing polar code. Moreover, this method can guide the way of using simpler short codes instead of long codes for the polar code construction.

TABLE 2. Error of effective information bit $K_{\max}$.

(*DSNR*,*N*)	(1,512)	(2,512)	(3,512)	(1,1024)	(2,1024)	(3,1024)
$K_{\max}\_MonteCarlo$	143	140	159	230	274	370
$K_{\max}\_proposed$	125	146	145	211	257	336
Error(%)	3.5%	1.2%	2.7%	1.9%	1.7%	3.3%

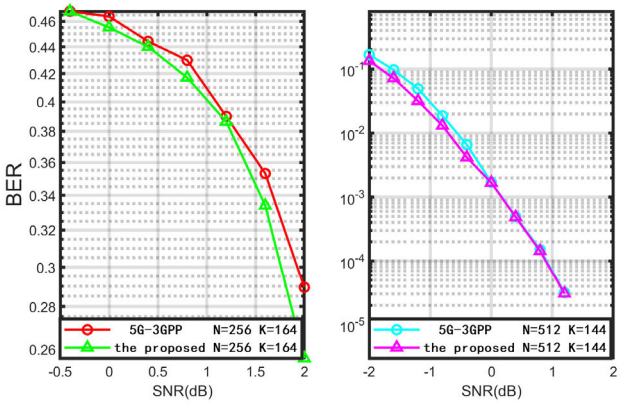

FIGURE 7. Comparison of BER performance of the proposed algorithm with the 5G-3GPP algorithm.

For example, the maximum value of ABLCR of the polar code with $N = 512$ is exactly the same as the polar code with $N = 1024$ even under different *Ks*. Therefore, the shorter code length of 512 can be used to replace the construction of the polar code with the length of 1024 within certain error probability ranges. Furthermore, in practical applications, apart from finding the optimal construction parameters, the proposed method is considerably efficient for parameter adjustment and selection.

In order to further verify the effectiveness of the proposed algorithm in practical applications, it is compared with the part of the polar code construction in the 5G standardization process of the 3rd generation partnership project (3GPP) in [36]. To facilitate comparison, the codeword length E is equal to N for the 5G standard algorithm for the downlink direction during the simulation, and the decoding algorithm uses the standard SC algorithm. The simulation results are shown in Fig.7 and Fig.8. When N is 256 and K is equal to 164, the proposed algorithm also achieves almost 0.05$\sim$ 0.2dB gain in *BER* and 0.1dB gain in *BLER* for different *SNR*s compared with the 5G-3GPP algorithm When the coding length N is 512 and K is equal to 144, the proposed algorithm achieves almost 0.1dB gain from -2 to 0 for *SNR*, and the performance of two algorithms is basically the same later in BER. Actually the proposed algorithm is always better than the 5G algorithm by almost 0.05dB in BLER So the

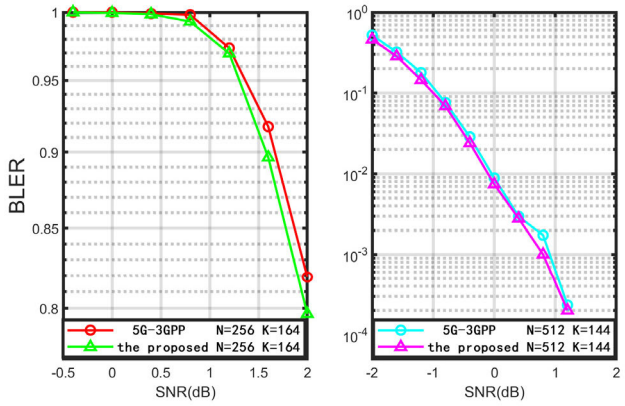

FIGURE 8. Comparison of BLER performance of the proposed algorithm with the 5G-3GPP algorithm.

overall performance of the proposed algorithm is better than the 5G-3GPP algorithm

VI. CONCLUSION

In this article, a method which constructs polar code by using optimal parameters is proposed. The proposed construction method can satisfy the minimum code length N and the best $DSNR$, and the specified error probability. In section V, the correctness of the algorithm was verified through simulation. In addition, the proposed algorithm can effectively determine the relationship between design parameters, performance and complexity which will benefit rate matching and punctured polar codes [37]–[40]. Furthermore, this method can also be extended to other concatenated polar codes to obtain the structure of the polar code with the optimal performance and lower complexity.

REFERENCES

[1] C. Yang, M. Zhan, Y. Deng, M. Wang, X. H. Luo, and J. Zeng, "Error-correcting performance comparison for polar codes, LDPC codes and convolutional codes in high-performance wireless," in *Proc. 6th Int. Conf. Inf., Cybern., Comput. Social Syst. (ICCSS)*, Sep. 2019, pp. 258–262.

[2] K. D. Rao, "Performance analysis of enhanced turbo and polar codes with list decoding for URLLC in 5G systems," in *Proc. IEEE 5th Int. Conf. for Converg. Technol. (I2CT)*, Mar. 2019, pp. 1–6.

[3] A. C. Vaz, C. Gurudas Nayak, and D. Nayak, "Performance comparison between turbo and polar codes," in *Proc. 3rd Int. Conf. Electron., Commun. Aerosp. Technol. (ICECA)*, Jun. 2019, pp. 1072–1075.

[4] Z. Mei, B. Dai, M. Johnston, and R. Carrasco, "Design of polar codes with single and multi-carrier modulation on impulsive noise channels using density evolution," 2017, *arXiv:1712.00983*. [Online]. Available: http://arxiv.org/abs/1712.00983

[5] P. Chen, B. Bai, Z. Ren, J. Wang, and S. Sun, "Hash-polar codes with application to 5G," *IEEE Access*, vol. 7, pp. 12441–12455, 2019.

[6] C. Sun, Z. Fei, C. Cao, X. Wang, and D. Jia, "Low complexity polar decoder for 5G Embb control channel," *IEEE Access*, vol. 7, pp. 50710–50717, 2019.

[7] L. Xiang, Z. B. Kaykac Egilmez, R. G. Maunder, and L. Hanzo, "Crc-aided logarithmic stack decoding of polar codes for ultra reliable low latency communication in 3gpp new radio," *IEEE Access*, vol. 7, pp. 28559–28573, 2019.

[8] O. Ïcan, R. Böhnke, and W. Xu, "Probabilistic shaping using 5G new radio polar codes," *IEEE Access*, vol. 7, pp. 22579–22587, 2019.

[9] M. Dhuheir and S. Ozturk, "Polar codes analysis of 5G systems," in *Proc. 6th Int. Conf. Control Eng. Inf. Technol. (CEIT)*, Oct. 2018, pp. 1–6.

[10] Z. B. Kaykac Egilmez, L. Xiang, R. G. Maunder, and L. Hanzo, "The development, operation and performance of the 5G polar codes," *IEEE Commun. Surveys Tuts.*, vol. 22, no. 1, pp. 96–122, 1st Quart., 2020.

[11] Q. Wang, W. Zhou, S. Zhang, and S. Wang, "Performance analysis of polar codes for wireless sensor networks," in *Proc. IEEE 9th Int. Conf. Electron. Inf. Emergency Commun. (ICEIEC)*, Jul. 2019, pp. 1–5.

[12] Y. Polyanskiy, H. V. Poor, and S. Verdu, "Channel coding rate in the finite blocklength regime," *IEEE Trans. Inf. Theory*, vol. 56, no. 5, pp. 2307–2359, May 2010.

[13] S. H. Hassani, K. Alishahi, and R. L. Urbanke, "Finite-length scaling for polar codes," *IEEE Trans. Inf. Theory*, vol. 60, no. 10, pp. 5875–5898, Oct. 2014.

[14] M. Mondelli, S. H. Hassani, and R. L. Urbanke, "Unified scaling of polar codes: Error exponent, scaling exponent, moderate deviations, and error floors," *IEEE Trans. Inf. Theory*, vol. 62, no. 12, pp. 6698–6712, Dec. 2016.

[15] E. Arkan, "A performance comparison of polar codes and reed-muller codes," *IEEE Commun. Lett.*, vol. 12, no. 6, pp. 447–449, Jun. 2008.

[16] E. Arikan, "Channel polarization: A method for constructing capacity-achieving codes for symmetric binary-input memoryless channels," *IEEE Trans. Inf. Theory*, vol. 55, no. 7, pp. 3051–3073, Jul. 2009.

[17] R. Mori and T. Tanaka, "Performance of polar codes with the construction using density evolution," *IEEE Commun. Lett.*, vol. 13, no. 7, pp. 519–521, Jul. 2009.

[18] R. Mori and T. Tanaka, "Performance and construction of polar codes on symmetric binary-input memoryless channels," in *Proc. IEEE Int. Symp. Inf. Theory*, Jun. 2009, pp. 1496–1500.

[19] I. Tal and A. Vardy, "How to construct polar codes," *IEEE Trans. Inf. Theory*, vol. 59, no. 10, pp. 6562–6582, Oct. 2013.

[20] M. Mondelli, S. H. Hassani, and R. Urbanke, "Construction of polar codes with sublinear complexity," in *Proc. IEEE Int. Symp. Inf. Theory (ISIT)*, Jun. 2017, pp. 1853–1857.

[21] G. He, J.-C. Belfiore, I. Land, G. Yang, X. Liu, Y. Chen, R. Li, J. Wang, Y. Ge, R. Zhang, and W. Tong, "Beta-expansion: A theoretical framework for fast and recursive construction of polar codes," in *Proc. IEEE Global Commun. Conf.*, Dec. 2017, pp. 1–6.

[22] C. Condo, S. A. Hashemi, and W. J. Gross, "Efficient bit-channel reliability computation for multi-mode polar code encoders and decoders," in *Proc. IEEE Int. Workshop Signal Process. Syst. (SiPS)*, Oct. 2017, pp. 1–6.

[23] Arikan, Erdal, and Emre Telatar, "On the rate of channel polarization," in *Proc. IEEE Int. Symp. Inf. Theory*, Jun. 2009, pp. 1493–1495.

[24] R. L. Dobrushin, "Mathematical problems in the Shannon theory of optimal coding of information," in *Proc. 4th Berkeley Symp. Math., Statist., Probab.*, vol. 1, 1961, pp. 211–252.

[25] S. H. Hassani, R. Mori, T. Tanaka, and R. L. Urbanke, "Rate-dependent analysis of the asymptotic behavior of channel polarization," *IEEE Trans. Inf. Theory*, vol. 59, no. 4, pp. 2267–2276, Apr. 2013.

[26] V. Strassen, "Asymptotische abschätzungen in Shannons informationstheorie," in *Proc. Trans. 3D Prague Conf. Inf. Theory*, 1962, pp. 689–723.

[27] W. Du, S. Zhang, and F. Ding, "Exploiting the UEP property of polar codes to reduce image distortions induced by transmission errors," in *Proc. IEEE/CIC Int. Conf. Commun. China (ICCC)*, Nov. 2015, pp. 1–5.

[28] P. Trifonov, "Efficient design and decoding of polar codes," *IEEE Trans. Commun.*, vol. 60, no. 11, pp. 3221–3227, Nov. 2012.

[29] D. Wu, Y. Li, and Y. Sun, "Construction and block error rate analysis of polar codes over AWGN channel based on Gaussian approximation," *IEEE Commun. Lett.*, vol. 18, no. 7, pp. 1099–1102, Jul. 2014.

[30] S.-Y. Chung, T. J. Richardson, and R. L. Urbanke, "Analysis of sum-product decoding of low-density parity-check codes using a Gaussian approximation," *IEEE Trans. Inf. Theory*, vol. 47, no. 2, pp. 657–670, 2001.

[31] R. M. Oliveira and R. C. de Lamare, "Puncturing based on polarization for polar codes in 5G networks," in *Proc. 15th Int. Symp. Wireless Commun. Syst. (ISWCS)*, Aug. 2018, pp. 1–5.

[32] L. Li, W. Song, and K. Niu, "Optimal puncturing of polar codes with a fixed information set," *IEEE Access*, vol. 7, pp. 65965–65972, 2019.

[33] V. Bioglio, F. Gabry, and I. Land, "Low-complexity puncturing and shortening of polar codes," in *Proc. IEEE Wireless Commun. Netw. Conf. Workshops (WCNCW)*, Mar. 2017, pp. 1–6.

[34] R. Wang and R. Liu, "A novel puncturing scheme for polar codes," *IEEE Commun. Lett.*, vol. 18, no. 12, pp. 2081–2084, Dec. 2014.

[35] H. Vangala, E. Viterbo, and Y. Hong, "A comparative study of polar code constructions for the AWGN channel," 2015, *arXiv:1501.02473*. [Online]. Available: http://arxiv.org/abs/1501.02473
[36] V. Bioglio, C. Condo, and I. Land, "Design of polar codes in 5G new radio," *IEEE Commun. Surveys Tuts.*, early access, Jul. 17, 2020, doi: 10.1109/COMST.2020.2967127.
[37] M. Mondelli, S. H. Hassani, I. Maric, D. Hui, and S.-N. Hong, "Capacity-achieving rate-compatible polar codes for general channels," in *Proc. IEEE Wireless Commun. Netw. Conf. Workshops (WCNCW)*, Mar. 2017, pp. 1–6.
[38] S.-N. Hong, D. Hui, and I. Maric, "Capacity-achieving rate-compatible polar codes," *IEEE Trans. Inf. Theory*, vol. 63, no. 12, pp. 7620–7632, Dec. 2017.
[39] M.-O. Jung and S.-N. Hong, "Construction of rate-compatible punctured polar codes using hierarchical puncturing," in *Proc. IEEE Int. Symp. Inf. Theory (ISIT)*, Jun. 2018, pp. 1859–1863.
[40] C. Schnelling, M. Rothe, N. Koep, R. Mathar, and A. Schmeink, "Efficient implementation of density evolution for punctured polar codes," *IEEE Access*, vol. 7, pp. 105909–105921, 2019.

HAICHAO SUN received the M.S. degree in control science and engineering from the Harbin Institute of Technology, Harbin, China, in 2012. He is currently pursuing the Ph.D. degree with the Changchun Institute of Optics, Fine Mechanics and Physics, Chinese Academy of Sciences, Changchun, China. His research interests include aerospace communications and image processing.

YANJIE WANG received the B.S. degree in computer science and applications from Jilin University, Changchun, China, in 1988, and the M.S. degree from the Changchun Institute of Optics, Fine Mechanics and Physics, Chinese Academy of Sciences, Changchun, in 1998. He is currently a Ph.D. Tutor and a Scientific Researcher with the Chinese Academy of Sciences. His research interest includes real-time image processing.

RUI TIAN received the B.S. degree in applied physics from Jilin University, Changchun, China, in 2002, and the Ph.D. degree in optical engineering from the Changchun Institute of Optics, Fine Mechanics and Physics, Chinese Academy of Sciences, Changchun, China, 2010. His research interest includes real-time image processing.

HONGWEI ZHAO received the M.S. degree in computer applications and the Ph.D. degree in mechanical manufacturing and automation from Jilin University, Changchun, China, in 1993 and 2001, respectively. He is currently a Ph.D. Tutor and a Scientific Researcher with Jilin University. His research interests cover embedded systems and cognitive computing.